American Mineralogist, Volume 72, pages 255–272, 1987

Variations in Mg/(Mg + Fe), F, and (Fe,Mg)Si = 2Al in pelitic minerals in the Ballachulish thermal aureole, Scotland

David R. M. Pattison*
Grant Institute of Geology, University of Edinburgh, West Mains Road, Edinburgh EH9 3JW, Scotland

Abstract

Three chemical variations in pelitic minerals have been examined through a well-defined sequence of prograde reactions in the 3-kbar thermal aureole surrounding the Devonian Ballachulish Igneous Complex, in Argyllshire, Scotland: (1) Mg/(Mg + Fe) partitioning between coexisting cordierite, biotite, and chlorite, (2) F in biotite, and (3) Si content, as controlled by the Tschermaks exchange [(Fe,Mg)Si = 2Al], in coexisting muscovite, biotite, and chlorite. The Mg/(Mg + Fe) variations are controlled mainly by the metamorphic grade via continuous reactions, the F variations mainly by primary bulk compositional differences, and the Si variations by a combination of the two.

Using a T-$X_{Fe\text{-}Mg}$ diagram constructed in the ideal pelitic system K_2O-FeO-MgO-Al_2O_3-SiO_2-H_2O, the theoretical prediction of the movement of Mg/(Mg + Fe) tie lines through a sequence of continuous reactions in both quartz-bearing and quartz-absent assemblages fits well with the measured compositions, with two major exceptions: specimens that come from graphitic slates, which contain minerals more magnesian than predicted, and specimens that contain biotite with significant F (>0.7 wt%), which are also anomalously magnesian. The first exception is due to the lowering of a_{H_2O} due to the presence of C-bearing fluid species, which shifts the stability of some of the reactions to more Mg-rich compositions, whereas the second is due to the stabilizing effect of F on Mg-rich biotite.

The Tschermaks exchange [(Fe,Mg)Si = 2Al] operates sympathetically in coexisting muscovite, biotite, and chlorite throughout a wide range of assemblages. This pattern highlights the importance of treating $(Fe,Mg)_{-1}Si_{-1}Al_2$ as a general exchange vector that operates in all amenable phases (e.g., mica) in an analogous fashion to the sympathetic Fe-Mg variations in coexisting ferromagnesian phases. Reactions involving (Fe,Mg)Si = 2Al may be evaluated using Schreinemakers analysis, leading to the construction of P-T and isobaric T-$X_{Al\text{-}Si}$ diagrams. The application of T-$X_{Al\text{-}Si}$ diagrams to assemblages from Ballachulish succinctly accounts both for the observed distribution of biotite-bearing and biotite-absent regional assemblages and for the measured variations in (Fe,Mg)Si = 2Al in a variety of contact metamorphic and regional assemblages.

Introduction

One of the main advantages of examining metamorphic processes in contact metamorphic aureoles around igneous bodies is that they represent relatively simple geologic settings, without the added complexities of polyphase deformation and temporal variations in pressure, temperature, and fluid movement that are all a part of dynamic regional metamorphism.

This paper describes the most conspicuous chemical variations of pelitic minerals in the thermal aureole surrounding the Ballachulish Igneous Complex, situated in the West Central Highlands in Argyllshire, Scotland. The Ballachulish Igneous Complex is a well-exposed Devonian composite pluton (8 × 4.5 km) emplaced in a sequence of Dalradian metasedimentary rocks that were deformed and metamorphosed to lower greenschist facies conditions during the Cambrian-Ordovician Caledonian orogeny. The chemical variations discussed in this paper include (1) the Mg/(Mg + Fe) variations between coexisting chlorite, biotite, and cordierite going through a prograde sequence of continuous and discontinuous reactions, which are illustrated and summarized in Figure 1 and Table 1, (2) the variation of F content in biotite and the influence it has on the Fe-Mg compositions of coexisting cordierite and biotite, and (3) the variation in the Si content of coexisting chlorite, muscovite, and biotite in a variety of regional and contact metamorphic assemblages. The variation in Si content is an indication of the extent of Tschermaks exchange [(Fe,Mg)Si = 2Al] within these minerals.

The broad range of assemblages and the well-defined sequence of prograde metamorphic zones in the Ballachulish aureole (Pattison, 1985; Pattison and Harte, 1985)

* Present address: Department of the Geophysical Sciences, University of Chicago, 5734 South Ellis Avenue, Chicago, Illinois 60637, U.S.A.

0003–004X/87/0304–0255$02.00

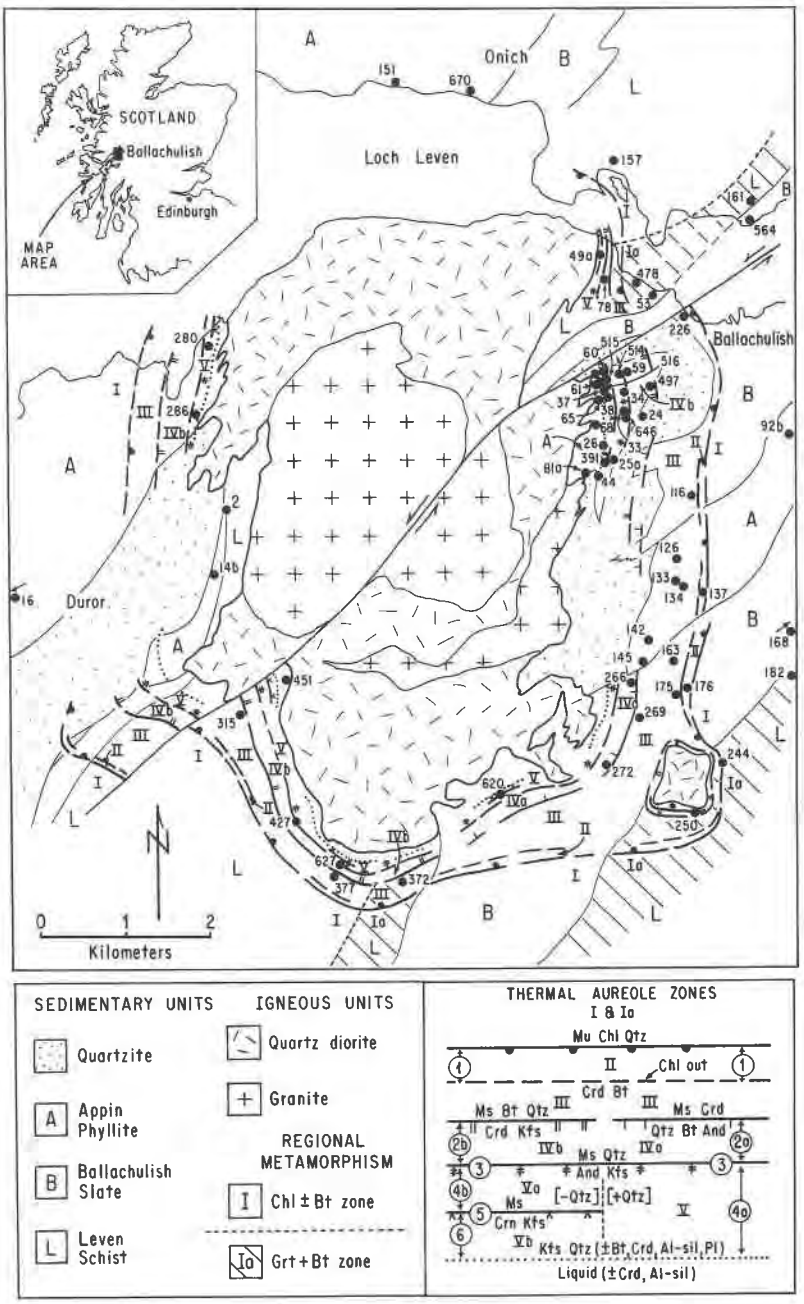

Fig. 1. Simplified geology, location of analyzed specimens and thermal aureole zones in pelitic rocks around the Ballachulish Igneous Complex (refined from Fig. 1 of Pattison and Harte, 1985). For clarity, only quartzite and the three main pelitic units discussed in the paper are illustrated.

provide an excellent controlled setting in which to assess some of the causes and effects of these chemical variations. Using a T-$X_{Fe\text{-}Mg}$ diagram, the theoretical prediction of the movement of Mg/(Mg + Fe) tie lines between coexisting cordierite, biotite, and chlorite passing through the continuous reactions of Table 1 is tested against the measured Mg/(Mg + Fe) compositions of these minerals in 60 specimens. Because the metamorphic grade in the aureole represents essentially isobaric heating, significant deviations from the predicted pattern can be used to identify the influence of minor element substitutions, e.g., F in biotite (see below).

Two of the most important aspects of this paper are (1) the routine analysis of the F content of biotite through a well-defined contact metamorphic sequence of pelitic assemblages and (2) the assessment of sympathetic variations with grade of (Fe,Mg)Si = 2Al between coexisting chlorite, muscovite, and biotite in *specific* regional and

TABLE 1. Summary of contact metamorphic zones and related continuous and discontinuous reactions

Zone	Subzone	Occurrence	Assemblage	Reaction**	Reaction no.	KFMASH† variance
I*	I	All units	Ms + Chl + Qtz ± Bt		—	3
	Ia	Leven Schist	Ms + Qtz + Bt + *Grt* ± Chl	Ms + 3Chl + 3Qtz = 4Grt + Bt + 12H_2O	—	2
II		All units	Ms + Chl + Qtz + *Crd* + *Bt*	Ms + Chl + 2Qtz = Crd + Bt + 3.5H_2O	1	2
III		All units	Ms + Qtz + Crd + Bt	Chl reacted out from zone II	—	3
IV	IVa	Ballachulish Slate	Ms + Qtz + Crd + Bt + *And*	2Ms + 3Crd = 7Qtz + 8And + 2Bt + 1.5H_2O	2a	2
	IVb	Leven Schist, Appin Phyllite	Crd + Bt + *Kfs* ± Ms ± Qtz	6Ms + 2Bt + 15Qtz = 3Crd + 8Kfs + 6.5H_2O	2b	2
—	—	All units	Ms + Qtz + *And* + *Kfs* + Crd + Bt	Ms + Qtz = And + Kfs + H_2O	3	1
V	V	Quartz-present pelites	*Qtz* + *And* + *Kfs* + Crd + Bt	9Qtz + 2Bt + 6And = 3Crd + 2Kfs + 0.5H_2O	4a	2
	Va		*Ms* + *And* + *Kfs* + Crd + Bt	9Ms + 3Crd = 2Bt + 15 And + 7 Kfs + 8.5H_2O	4b	2
	—	Quartz-absent pelites	Ms + *Crn* + And + Kfs + Crd + Bt	Ms = Crn + Kfs + H_2O	5	1
	Vb		Crn + And + Kfs + Crd + Bt	2Bt + 15And = 9Crn + 3Crd + 2Kfs + 0.5H_2O	6	2

* Zone I represents *regional-grade* assemblages, developed prior to contact metamorphism.
** Cordierite is assumed to contain 0.5 mol of structurally bound H_2O [i.e., $(Fe,Mg)_2Al_4Si_5O_{18}\cdot 0.5H_2O$]. This is a mean value for the *P-T* range in the Ballachulish aureole (3 kbar, 500–700°C), taken from the cordierite H_2O-content study of Mirwald and Schreyer (1977).
† The variance of the assemblages assumes the presence of a hydrous fluid phase.

contact metamorphic assemblages. The analysis of the F content of biotite through the aureole shows whether metamorphic grade or primary bulk compositional variation is the major factor in controlling its concentration (see Valley et al., 1982). The assessment of sympathetic variations in (Fe,Mg)Si = 2Al in specific assemblages is important because it is often overlooked that the Si content of coexisting chlorite, muscovite, and biotite varies according to the assemblage in which the minerals coexist, as is well known for Mg/(Mg + Fe) variation (see below and Thompson, 1976). The observed (Fe,Mg)Si = 2Al variations highlight the importance of treating this exchange as a reaction vector in the sense of Thompson (1982a, 1982b) and leads to the construction of T-$X_{Al\text{-}Si}$ diagrams that succinctly account for these variations.

GEOLOGIC SETTING

The Ballachulish Igneous Complex, one of numerous posttectonic plutonic bodies emplaced throughout the Scottish Caledonides at the end of the Caledonian orogeny, is a composite, calc-alkaline "I-type" pluton (Harmon, 1983). The complex consists of an outer, gray quartz diorite, containing abundant sedimentary xenoliths at its margins, which is crosscut by an inner, pink monzogranite (Troll and Weiss, 1984). Radiometric dating of hornblende and biotite of the outer quartz diorite gives an Early Devonian closure age of 402 ± 18 Ma (Miller and Brown, 1965; Brown et al., 1968). The average emplacement temperature of the outer quartz diorite is estimated at 1050°C, whereas the inner granite emplacement temperature is estimated at 800–850°C (Troll and Weiss, 1984; Weiss, 1986).

Three major pelitic groups enter the Ballachulish aureole (see Fig. 1): (1) graphitic, locally silty, pyrite- and/or pyrrhotite-bearing slates of the Ballachulish Slate, the Ballachulish Slate–Appin Quartzite Transition Series and the Cuil Bay Slate (B), (2) pelitic to semipelitic metasedimentary rocks of the Appin Phyllite (A), and (3) phyllites, semipelites, striped siltstones, and dirty quartzites of the Leven Schist (L). The Leven Schist is defined here as in Bailey and Maufe (1960), although Litherland (1980) has reassigned some of the units into a more detailed, revised stratigraphy.

Each of these units is grossly similar lithologically and geochemically and can be reliably identified at all grades in the aureole. The mean and range of the bulk Mg/(Mg + Fe) variation of the three units, based on specimens that contain a low modal abundance of oxide and sulfide minerals, are as follows: Ballachulish Slate, 0.50, 0.43–0.61, n = 9; Appin Phyllite 0.53, 0.38–0.71, n = 16; and Leven Schist, 0.38, 0.28–0.47, n = 15. Overall, the Leven Schist is more Fe-rich than the Appin Phyllite and Ballachulish Slate, and the Ballachulish Slate is distinguished by being the only graphitic unit.

One major deformation has affected the metasedimentary rocks in the area [D_1 in the terminology of Roberts (1976) and Treagus (1974)], which has produced the major NE–SW oriented structures. Regional metamorphism, approximately coeval with the deformation, increases in grade from the northwest to southeast, as manifested by

TABLE 2. Mineral assemblages of analyzed specimens

Zone	Unit	Rock	Qtz	Chl	Ms	Grt*	Bt	Crd	Kfs	And	Sil	Crn	Ilm	Gr
I	B	D564	X	X	X								X	X
	A	16	X	X	X		X						X	
	A	92b	X	X	X		X						?	
	A	151	X		X		X						X	
	A	670	X	X	X		X						X	
	L	157**	X	X	X								X	
	L	168†	X	X	X		X						X	
	L	182†	X	X	X		X						X	
Ia (+Grt)*	L	53	X	X	X	X	X						X	
	L	161	X	X	X	X	X						X	
	L	478	X	X	X	X	X						X	
II	B	176	X	X	X		X	P						X
	A	137	X	X	X		X	P					X	
III	B	116	X		X		X	P					?	X
	B	163	X		X		X	X					X	X
	B	175	X		X		X	X					X	X
	B	226	X		X		X	X					X	X
	B	269	X		X		X	X					X	X
	A	126	X		X		X	X					X	
	A	133	X		X		X	P					X	
	A	134	X		X		X	X					X	
	A	142	X		X		X	P						
	A?	145	X		X		X	P					X	X
	L	315	X		X		X	X					X	
	L	377	X		X		X	X					X	
IVa‡	B	266	X		X		X	X		X			X	X
	B	272	X		X		X	X		X			X	X
IVb‡	A	24	X				X	X	X				X	
	A	59			X		X	X	X				X	
	A	497	X		X		X	X	X				X	
	L	78	X				X	X	X				?	
R(3)	L	250	X		X		X	X	X	X			X	
	L	427	X		X		X	X	X	X	X		X	
	L	627	X		X		X	X	X	X			X	
V	A	14b††	X				X	X	X				X	
	A	26††	X				X	X	X				X	
	A	33††	X				X	X	X				X	
	A	34(1)	X				X	X	X	X	X		X	
	A	34(2)††	X				X	X	X				X	
	A	38††	X				X	X	X				X	
	A	81††	X				X	X	X				X	
	A	280††	X				X	X	X				X	
	A	286††	X				X	X	X				X	
	A	515	X				X	X	X	X	X		X	
	L	2	X					X	X	X	X		X	
Va§	A	25a			X		X	X	X	X	X			
	A	514			X		X	X	X	X	X			
	A	516					X	X	X	X	X			
	A	646			X		X	X	X	X				
R5	A	391			X		X	X	X	X		X		
	A	620			X		X	X	X	X	X	X	X	
Vb	A	37					X	X	X	X		X	X	
	A	44					X	X	X	X	X	X	X	
	A	60					X	X	X	X	X	X	X	
	A	61					X	X	X	X		X	X	
	A	63b					X	X	X	X	X	X	X	
	A	65					X	X	X	X	X	X	X	
	A	68					X	X	X	X	X	X	X	
	L	49a					X	X	X	X	X	X	X	
	L	451					X	X	X	X	X	X	X	

Note: Refer to Fig. 1 and Table 1 for the sequence of zones. All specimens contain plagioclase (usually ≪5% modally), and at least some secondary muscovite; tourmaline, apatite, zircon, rutile, and minor sulfide may be present. B = Ballachulish Slate. A = Appin Phyllite. L = Leven Schist. P = pinitized, or altered, cordierite. R3, R5: univariant assemblages Ms + Qtz + Al_2SiO_5 + Kfs + Crd + Bt and Ms + Crn + Kfs + Al_2SiO_5 + Crd + Bt, corresponding to univariant Reactions 3 and 5, respectively.

* Garnet is regional in origin.

** Assemblage contains epidote.

† Assemblage contains epidote and dolomite.

‡ These two zones, together which define zone IV, are not sequential in grade but are developed in rocks of different bulk composition (see Table 1 and Pattison and Harte, 1985).

†† Specimens that are spatially within zone V but contain assemblages developed in zone IVb (Reaction 2b; see text).

§ These zones are exclusively developed in quartz-absent rocks, but occur spatially within and define subzones within zone V, in which quartz is present (see Table 1 and Pattison and Harte, 1985).

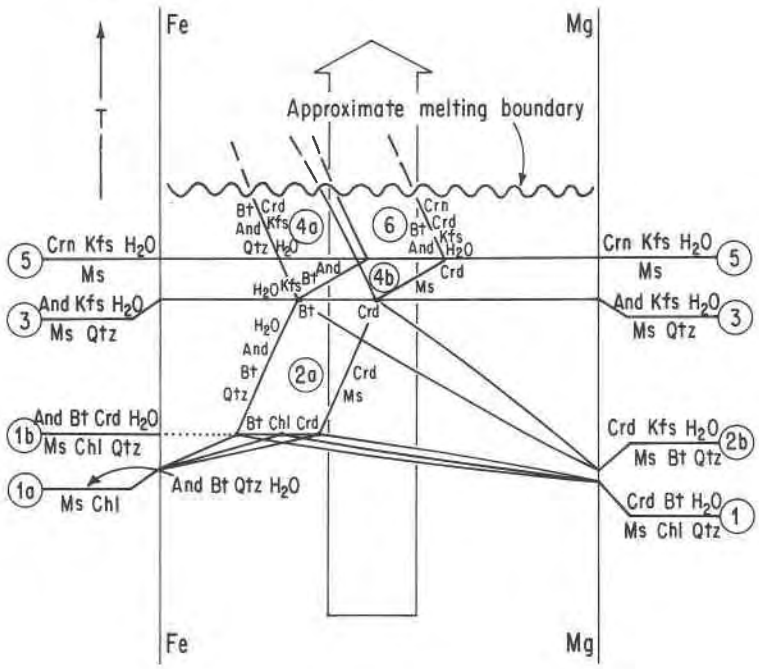

Fig. 2. Schematic isobaric T-$X_{Fe\text{-}Mg}$ diagram for the divariant reactions in the Ballachulish aureole (see Table 1 for the correspondence of the thermal aureole zones with the reactions). The broad arrow encompasses the bulk of the Mg/(Mg + Fe) compositional variation of the pelites in the aureole.

the development of garnet in pelites with Chl + Ms ± Bt via the simplified reaction Ms + Chl + Qtz = Grt + Bt + H_2O (see Fig. 1). The restricted occurrence of the garnet zone to the Leven Schist, as seen in Figure 1, is due to the more Fe-rich bulk composition of this unit as compared to the slates and the Appin Phyllite (Pattison, 1985). Regional metamorphic conditions are estimated to be 6–8 kbar and ranging from 500°C at the first appearance of garnet to 580°C in the garnet zone in the southeast corner of the area (Pattison, 1985).

The best estimate of pressure in the aureole is 3.0 ± 0.5 kbar, based on the P-T-$X_{Fe\text{-}Mg}$-X_{H_2O} calibration of the reactions in Table 1, and the application of numerous recently calibrated geobarometers (Pattison, 1985). This pressure is independently confirmed by S. Heuss-Assbichler (pers. comm., 1986) from P-T-X_{CO_2} calibration of carbonate reactions in the aureole.

Sample strategy and selection of analyses

The compositions of minerals from 60 selected specimens (see Fig. 1) were analyzed by wavelength-dispersive spectrometry on a Cambridge Instruments Microscan Mark 5 electron microprobe at the Grant Institute of Geology, Edinburgh University. All analyses were performed with a focused beam of 1–2-μm diameter, with a penetration of 2–3 μm, at an accelerating potential of 20 kV and probe current of 30 nA. Raw X-ray counts were collected and run through an on-line computer program for ZAF corrections after Sweatman and Long (1969), using the absorption coefficients of Heinrich (1966).

Specimens were selected from each contact metamorphic zone, in addition to regional zones. An attempt was made to have at least two representatives of each zone and to analyze specimens from all of the three pelitic units (see above). The most serious practical limitations were the high proportion of specimens that contain pinitized cordierite, and the difficulty in obtaining uncontaminated analyses in the phyllites and hornfelses, both of which are very fine grained. This latter problem is particularly acute when analyzing muscovite, chlorite, and biotite; for example, only a very small amount of quartz, chlorite, feldspar, or biotite contamination leads to an inaccurate muscovite analysis with a falsely high apparent phengitic component. All analyses showing evidence of even slight contamination were discarded, which typically left 3 to 6 good analyses of each mineral from each rock (with allowance for core-rim variations).

Table 2 lists the mineral assemblages of each of the probed specimens, and Table 3 lists selected chemical data for chlorite, muscovite, biotite, and cordierite through the different zones. These data represent the *average* values of each mineral in the rock, with core-rim variations being noted. A table of full single, representative mineral analyses from each rock may be obtained separately.[1] All mineral abbreviations follow the scheme of Kretz (1983).

Mg/(Mg + Fe) variations

Figure 1 illustrates the distribution of the prograde metamorphic zones in the Ballachulish aureole. In Table 1, these zones are related to a series of continuous and

[1] To obtain a copy of the representative mineral analyses, order Document AM-87-331 from the Business Office, Mineralogical Society of America, 1625 I Street, N.W., Suite 414, Washington, D.C. 20006, U.S.A. Please remit $5.00 in advance for the microfiche.

TABLE 3. Variation with grade of selected chemical data of muscovite, chlorite, biotite, and cordierite

			Muscovite			Chlorite			Biotite					Cordierite
Zone	Unit	Rock	Si	ΣX^{2+}	Mg/(Mg + Fe)	Si	ΣX^{2+}	Mg/(Mg + Fe)	Si	Al	Ti	Mg/(Mg + Fe)	F (wt%)	Mg/(Mg + Fe)
I	B	D564	3.13	0.31	0.62	2.63	4.66	0.61	—	—	—	—	—	—
	A	16	3.32	0.44	0.64	2.74	4.59	0.54	2.87	1.42	0.11	0.53	0.5	—
	A	92b	3.27	0.49	0.59	2.76	4.75	0.75	2.88	1.36	0.08	0.72	0.3	—
	A	151	3.30	0.52	0.49	—	—	—	2.78	1.54	0.08	0.58	0.3	—
	A	670	3.23	0.47	0.43	2.70	4.69	0.52	2.82	1.52	0.08	0.48	nd	—
	L	157	3.19	0.35	0.40	2.61	4.64	0.40	—	—	—	—	—	—
	L	168	3.26	0.60	0.56	2.83	4.95	0.75	2.83	1.35	0.07	0.72	0.7	—
	L	182	3.28	0.48	0.50	2.70	4.77	0.67	—	—	—	—	—	—
Ia (+Grt)	L	53	3.27	0.32	0.53	2.62	4.61	0.42	2.77	1.62	0.14	0.39	0.3	—
	L	161	3.15	0.27	0.50	2.61	4.60	0.41	2.72	1.62	0.12	0.38	0.2	—
	L	478	3.21	0.30	0.47	2.66	4.56	0.40	2.78	1.66	0.11	0.37	0.1	—
II	B	176	3.21	0.26	0.67	2.67	4.57	0.63	2.71	1.73	0.07	0.61	nd	—
	A	137	3.14	0.24	0.43	2.63	4.39	0.41	2.69	1.88	0.07	0.37	nd	—
III	B	116	3.18	0.23	0.72	—	—	—	2.66	1.85	0.04	0.60	0.8	—
	B	163	3.17	0.19	0.61	—	—	—	2.69	1.81	0.07	0.53	0.4	0.64
	B	175	3.17	0.38	0.54	—	—	—	2.71	1.77	0.07	0.57	0.5	0.69
	B	226	3.14	0.18	0.59	—	—	—	2.58	1.83	0.08	0.46	nd	0.59
	B	269	3.09	0.31	0.51	—	—	—	2.67	1.79	0.12	0.46	0.5	0.60
	A	126	3.23	0.36	0.65	—	—	—	2.75	1.69	0.07	0.54	0.3	0.64
	A	133	3.21	0.35	0.66	—	—	—	2.81	1.62	0.09	0.59	0.4	—
	A	134	3.14	0.39	0.55	—	—	—	2.73	1.75	0.08	0.50	0.2	0.62
	A	142	3.26	0.19	0.80	—	—	—	2.85	1.56	0.08	0.73	0.3	—
	A	145	3.13	0.19	0.57	—	—	—	2.57	1.88	0.13	0.43	0.3	—
	L	315	3.17	0.23	0.42	—	—	—	2.64	1.80	0.14	0.30	0.1	0.46
	L	377	3.12	0.17	0.49	—	—	—	2.64	1.87	0.07	0.37	nd	0.49
IVa	B	266	3.12	0.17	0.65	—	—	—	2.63	1.80	0.03	0.45	0.5	0.54
	B	272	3.14	0.14	0.67	—	—	—	2.71	1.74	0.13	0.49	0.7	0.57
IVb	A	24	3.06	0.16	0.53	—	—	—	2.68	1.77	0.15	0.44	nd	0.57
	A	59	3.18	0.33	0.54	—	—	—	2.63	1.60	0.14	0.56	1.2	0.68
	A	497	—	—	—	—	—	—	2.83	1.56	0.12	0.62	nd	0.70
	L	78	3.03	0.12	0.41	—	—	—	2.60	1.87	0.15	0.34	0.2	0.49
R(3)	L	250	3.06	0.27	0.26	—	—	—	2.66	1.73	0.19	0.36	0.3	0.50
	L	427	3.08	0.12	0.55	—	—	—	2.71	1.79	0.12	0.38	0.5	0.50
	L	627	3.08	0.17	0.55	—	—	—	2.68	1.80	0.10	0.41	0.6	0.49

TABLE 3.—*Continued*

Zone	Unit	Rock	Muscovite			Chlorite			Biotite					Cordierite
			Si	ΣX^{2+}	Mg/(Mg + Fe)	Si	ΣX^{2+}	Mg/(Mg + Fe)	Si	Al	Ti	Mg/(Mg + Fe)	F (wt%)	Mg/(Mg + Fe)
V	A	14b*	—	—	—	—	—	—	2.63	1.63	0.27	0.42	0.3	0.57
	A	26*	—	—	—	—	—	—	2.67	1.68	0.20	0.57	0.2	0.71
	A	33*	—	—	—	—	—	—	2.78	1.57	0.15	0.71	0.6	0.79
	A	34(1)	—	—	—	—	—	—	2.62	1.93	0.09	0.36	0.1	0.51
	A	34(2)*	—	—	—	—	—	—	2.60	1.83	0.15	0.42	0.1	0.54
	A	38*	—	—	—	—	—	—	2.69	1.66	0.20	0.45	0.4	0.65
	A	81a*	—	—	—	—	—	—	2.70	1.61	0.21	0.50	0.4	0.64
	A	280*	—	—	—	—	—	—	2.66	1.77	0.19	0.36	0.4	0.51
	A	515	—	—	—	—	—	—	2.69	1.68	0.15	0.45	0.8	0.59
	L	2	—	—	—	—	—	—	2.62	1.73	0.21	0.30	0.3	0.46
Va	A	25a	—	—	—	—	—	—	2.68	1.75	0.09	0.73	1.4	0.78
	A	514	3.06	0.28	0.35	—	—	—	2.63	1.65	0.15	0.54	1.2	0.71
	A	516	—	—	—	—	—	—	2.64	1.68	0.14	0.53	1.2	0.62
	A	646	3.06	0.19	0.65	—	—	—	2.61	1.79	0.14	0.58	0.7	0.70
R(5)	A	391	3.09	0.12	0.66	—	—	—	2.60	1.79	0.14	0.60	0.6	0.71
	B?	620	3.17	0.30	0.48	—	—	—	2.62	1.72	0.17	0.50	0.3	0.68
Vb	A	37	—	—	—	—	—	—	2.66	1.77	0.14	0.47	0.7	0.56
	A	44	—	—	—	—	—	—	2.61	1.87	0.19	0.47	0.3	0.61
	A	60	—	—	—	—	—	—	2.64	1.72	0.21	0.41	0.3	0.60
	A	61	—	—	—	—	—	—	2.68	1.65	0.14	0.58	0.3	0.70
	A	63b	—	—	—	—	—	—	2.66	1.67	0.12	0.77	1.5	0.82
	A	65	—	—	—	—	—	—	2.66	1.75	0.18	0.37	0.3	0.52
	A	68	—	—	—	—	—	—	2.69	1.65	0.15	0.56	0.3	0.68
	L	49a	—	—	—	—	—	—	2.65	1.75	0.20	0.47	0.2	0.58
	L	451	—	—	—	—	—	—	2.61	1.81	0.16	0.32	0.5	0.42
See footnotes			3.07† (3.03–3.11)	0.21† (0.12–0.30)	—	2.66†† (2.54–2.77)	4.62†† (4.47–4.82)	—	2.66§ (2.59–2.75)	1.67§ (1.48–1.87)	0.27§ (0.09–0.37)	—	0.3§ (nd–0.6)	—

Note: Cations calculated for muscovite and biotite based on 11 oxygens. Cations calculated for chlorite based on 14 oxygens. Tables of complete mineral analyses are available from the Business Office of *The American Mineralogist* (see footnote 1 in text).

* Specimens that are spatially within zone IV but contain assemblages developed in zone IVb (Reaction 2b; see text).

† Average secondary muscovite from high-grade rocks (26 rocks).

†† Average secondary chlorite from high-grade rocks (21 rocks).

§ Average biotite from the zone of partial melting (35 rocks).

discontinuous reactions in the model pelitic system K_2O-FeO-MgO-Al_2O_3-SiO_2-H_2O (KFMASH), which are illustrated in a schematic isobaric T-$X_{Fe\text{-}Mg}$ diagram in Figure 2. Mineral zones are indicated by Roman numerals, and reactions are indicated by Arabic numerals. The table and figures come from Pattison and Harte (1985), in which the description of the mineral zones, their relation to the reactions of Table 1, and the inferred presence of a hydrous fluid phase during metamorphism are discussed in detail.

In this section, the theoretical constraints of the T-$X_{Fe\text{-}Mg}$ diagram are evaluated against the measured Mg/(Mg + Fe) compositions of coexisting cordierite, biotite, and in zone II, chlorite. If the theoretical diagram accurately predicts the chemical variations of the analyzed specimens from the different zones, the following conditions should be met:

1. Above Reaction 1 (Ms + Chl + Qtz = Crd + Bt + H_2O), through which all pelites of normal composition (i.e., excluding those of very Fe-rich composition) pass, more Fe-rich pelites will encounter Reaction 2a (Ms + Crd = Qtz + Bt + Al_2SiO_5 + H_2O), while more Mg-rich pelites will encounter Reaction 2b (Ms + Bt + Qtz = Crd + Kfs + H_2O). The compositions of coexisting cordierite and biotite, passing through Reaction 2a (zone IVa), will move to more Mg-rich compositions, while those passing through Reaction 2b (zone IVb) will become more Fe-rich. Both reactions converge in Mg/(Mg + Fe) until they terminate against Reaction 3 (Ms + Qtz = Kfs + Al_2SiO_5 + H_2O), where pelites from either of the zones that still contain the complete divariant assemblages should contain cordierite and biotite with the same Mg/(Mg + Fe) ratios. Below the Ms + Qtz breakdown, there should be no overlap in Mg/(Mg + Fe) between pelites of zones IVa and IVb (i.e., all pelites of zone IVa should be more Fe-rich than any of zone IVb).

2. Above Reaction 3, depending upon whether Ms or Qtz is consumed, pelites enter either Reactions 4a (Bt + Qtz + Al_2SiO_5 = Crd + Kfs + H_2O) or 4b (Ms + Crd = Bt + Al_2SiO_5 + Kfs + H_2O). Using similar arguments as above, there should be no overlap in Mg/(Mg + Fe) of pelites in the two zones, with all of the pelites in zone V (Reaction 4a) containing cordierite and biotite more Fe-rich than in zone Va (Reaction 4b). In quartz-absent pelites that pass through Reaction 4b with muscovite still present, Reaction 5 (Ms = Crn + Kfs + H_2O) is encountered, followed upgrade by Reaction 6 (Bt + As = Crn + Crd + Kfs + H_2O). On Reaction 5, the Mg/(Mg + Fe) ratios of the cordierite and biotite should be at their maximum; the Mg/(Mg + Fe) ratios of these minerals increase during passage through Reaction 4b toward Reaction 5 and decrease during passage through Reaction 6 away from Reaction 5.

Trivariant assemblages

Throughout the aureole, the most widespread assemblages are the assemblages Ms + Bt + Crd + Qtz at low grades (up to and including zone III) and Crd + Bt + Qtz + Kfs at medium and high grades (above zone III). It is assumed that there was additionally a hydrous fluid phase with high a_{H_2O} present during prograde metamorphism (see Pattison and Harte, 1985, p. 9), so that these assemblages are therefore trivariant in the model KFMASH system. The assemblage Crd + Bt + Qtz + Kfs may be developed during passage through either Reaction 2b (Ms + Bt + Qtz = Crd + Kfs + H_2O), with the consumption of Ms, or Reaction 4a (Qtz + Bt + Al_2SiO_5 = Crd + Kfs + H_2O), with the consumption of Al_2SiO_5. By far, most specimens containing this assemblage are quartz-rich semipelites that originally contained a smaller amount of muscovite than did the pelitic specimens. Combined with the textural evidence described in Pattison and Harte (1985), it is clear that this assemblage was developed during passage through Reaction 2b with the consumption of Ms. This assemblage is stable throughout all succeeding zones up to the onset of partial melting. Thus, regardless of where in the higher-grade zones this assemblage is collected, the Mg/(Mg + Fe) composition of its cordierite and biotite will have been determined during its passage through Reaction 2b (assuming that the change in Fe-Mg partitioning between cordierite and biotite with increasing temperature is insignificant; see below).

Zones II and III

Figure 3a illustrates the compositions of cordierite, chlorite, and biotite from zone II (Ms + Chl + Bt + Crd + Qtz) and cordierite and biotite from zone III (Ms + Crd + Bt + Qtz), in an AFM diagram projected from Ms, Qtz, and H_2O (A = Al_2O_3 − $3K_2O$, F = FeO + MnO, M = MgO). Unfortunately, no complete Chl + Bt + Crd assemblages with fresh cordierite and primary chlorite were analyzed. Primary chlorite is texturally characterized by occurring in well-defined tabular grains of uniform grain size (100–200 μm) that grow parallel to the schistosity of the slates and phyllites, in contrast to secondary chlorite, which is of more variable and usually coarser grain size, is less tabular, and is often a conspicuous alteration product of cordierite and biotite. Nevertheless, it is clear from Figure 3a that the Mg/(Mg + Fe) composition of chlorite is intermediate between cordierite and biotite, but lies to the Fe-rich side of the cordierite-biotite tie line. This AFM topology is the same as found by Guidotti et al. (1975) in extremely Mg-rich compositions in regional rocks in Maine, by Evans and Speer (1984) in the Lilesville pluton aureole, and by Labotka et al. (1981) in the Rove Formation, Minnesota, demonstrating that Reaction 1 (Ms + Chl + Qtz = Crd + Bt + H_2O) begins in Mg-rich compositions and moves to more Fe-rich compositions throughout a large range of Mg/(Mg + Fe) compositional space. Supporting this topology is the weak Mg/(Mg + Fe) zonation of cordierite to slightly more Fe-rich rim compositions in specimens D269 and D377.

Zones IVa and IVb

Figure 3b illustrates in an AFM diagram projected from Kfs, Qtz, and H_2O the compositions of coexisting cordierite and biotite from zone IVb (Ms + Bt + Crd + Kfs + Qtz) and from the univariant assemblage Ms + Qtz + Kfs + Al_2SiO_5 + Crd + Bt (Reaction 3) (A = Al_2O_3 − K_2O, F = FeO + MnO, M = MgO). The Mg/(Mg + Fe) compositions of the three univariant specimens, collected from different parts of the aureole, define a fairly narrow range, which is consistent with their model univariance. With one exception (D78), the Mg/(Mg + Fe) ratios of cordierite and biotite are lower than those of the univariant assemblage, which is consistent with the theoretical arguments discussed above. The movement of tie lines to more Fe-rich compositions is further supported by the zonation of Mg/(Mg + Fe) in cordierite toward more Fe-rich rim compositions in specimens D24 and D33.

Figure 3c illustrates in an AFM diagram projected from Ms, Qtz, and H_2O the compositions of coexisting cordierite and biotites from zone IVa (Ms + Crd + Bt + Al_2SiO_5 + Qtz) and from the same univariant assemblage as Figure 3b. Although the theoretical migration of tie lines toward more Mg-rich compositions, as illustrated in Figure 2, is consistent with the zonation in cordierite to more Mg-rich rim compositions in D266, the absolute Mg/(Mg + Fe) values are *more* Mg-rich than those of the univariant assemblages. Because Reaction 2a (Ms + Crd = Qtz + Bt + Al_2SiO_5 + H_2O) terminates upgrade at Reaction 3 (Ms + Qtz = Kfs + Al_2SiO_5 + H_2O) (see Fig. 2), the Mg/(Mg + Fe) compositions of cordierite and biotite in theory should be *less* Mg-rich than those of the univariant assemblage.

Both of these specimens come from the graphitic Ballachulish Slate. The presence of graphite introduces CO_2 and CH_4 to the H_2O-rich vapor phase, lowering the a_{H_2O}; this has the dual effect of shifting the stability fields of the reactions to relatively more magnesian compositions and therefore preferentially favoring the stability of this assemblage relative to the zone IVb assemblage Ms + Bt + Qtz + Crd + Kfs (Pattison and Harte, 1985). This conclusion is based on quantitative calculations of the amount of shift in the reactions due to the presence of C-bearing fluid species (Pattison, 1985).

Zones V, Va, and Vb

Figure 3d illustrates the compositions of cordierite and biotite from zones V (Qtz + Bt + Crd + Al_2SiO_5 + Kfs) and Va (Ms + Bt + Crd + Al_2SiO_5 + Kfs). A modified AFM diagram, projected from Kfs, Al_2SiO_5, and H_2O is necessitated for these zones because quartz is no longer ubiquitous. The diagram is better described as an SFM projection, with S = SiO_2 + $6K_2O$ + Al_2O_3, F = FeO + MnO, and M = MgO. Two zone V specimens have Mg/(Mg + Fe) compositions less magnesian than those of the univariant assemblage Ms + Qtz + Kfs + Al_2SiO_5 + Crd + Bt, consistent with the theoretical pattern in Figure 2. One specimen, D515, is more magnesian than the univariant assemblage; this specimen contains ~0.8 wt% F.

In zone Va (Ms + Crd + Bt + Al_2SiO_5 + Kfs), all of the specimens have Mg/(Mg + Fe) ratios that are higher than the univariant assemblage, which is consistent with the movement of tie lines to more magnesian compositions during passage through Reaction 4b (Ms + Crd = Bt + Al_2SiO_5 + Kfs + H_2O) (see Fig. 2). Also plotted in Figure 3d are the two specimens containing the quartz-absent univariant assemblage Ms + Crn + Al_2SiO_5 + Crd + Bt + Kfs (Reaction 5). Unlike the three specimens containing the quartz-bearing univariant assemblage Ms + Qtz + Al_2SiO_5 + Crd + Bt + Kfs (Reaction 3), which defined a fairly narrow range of Mg/(Mg + Fe) in both biotite and especially cordierite, these quartz-absent univariant specimens show a greater range in Mg/(Mg + Fe). The more magnesian specimen of the two, D391, contains biotite with 0.6 wt% F.

With one exception, D516, all of the divariant specimens from zone Va contain cordierite and biotite approximately equal to or *more magnesian* than that of D620, the quartz-absent univariant assemblage containing biotite with minor F. This contradicts the theoretical prediction from Figure 2: because Reaction 4b terminates against univariant Reaction 5 (Ms = Cor + Kfs + H_2O), the Mg/(Mg + Fe) compositions of cordierite and biotite ideally should approach but not exceed those of the univariant assemblage. Notably, all of the zone Va specimens contain biotite with F contents greater than 0.7 wt%, with the most magnesian, D25a, containing biotite with the highest F content (1.4 wt%).

In Figure 3e, cordierite and biotite compositions from zone Vb (Bt + Al_2SiO_5 + Crn + Crd + Kfs) are plotted in an SFM diagram. With one exception, D63b, all of the specimens contain cordierite and biotite with less magnesian compositions than the quartz-absent univariant specimen D620, which is consistent with the theoretical movement of tie lines to more Fe-rich compositions during passage through continuous Reaction 6 (Bt + Al_2SiO_5 = Crn + Crd + Kfs + H_2O). Predictably, D63b contains biotite with considerable F (1.4 wt%).

Influence of F

It is well known that F stabilizes Mg-biotite relative to Fe-biotite owing to Fe-F avoidance in biotite (see Munoz, 1984, for a review). The F contents in the biotites from the Ballachulish aureole represent site occupancies up to 0.35 out of two hydroxyl sites (F/F + OH = 0.18). In zones V, Va, and Vb, there is a correlation between high F content of biotite and anomalously magnesian compositions of coexisting cordierite and biotite. If only specimens that contain biotite with low (< 0.5 wt%) F are examined, the Mg/(Mg + Fe) compositions of cordierite and biotite from these zones fit with the theoretical compositional trends illustrated in Figure 2.

It may be concluded that it is the F in biotites that

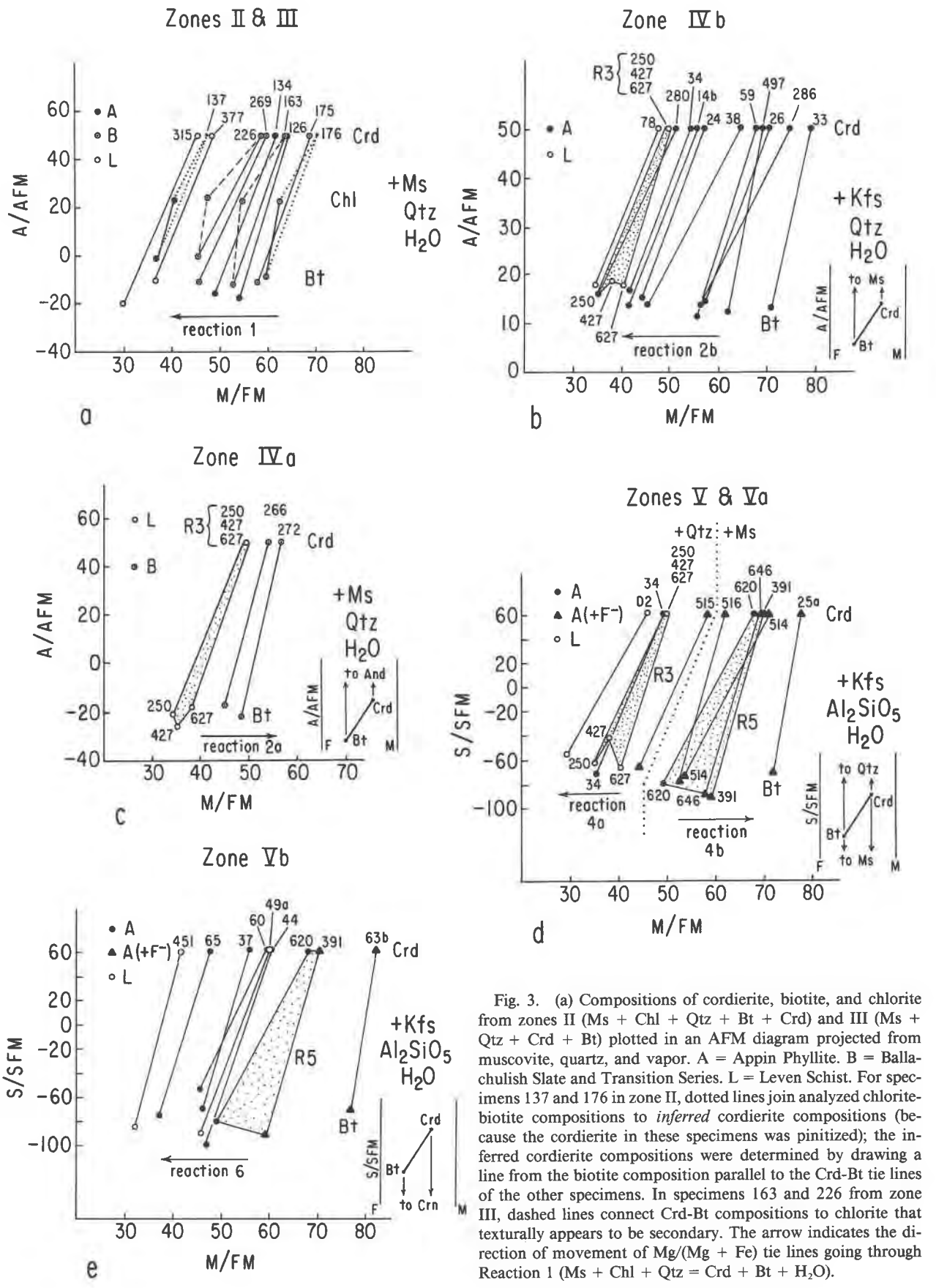

Fig. 3. (a) Compositions of cordierite, biotite, and chlorite from zones II (Ms + Chl + Qtz + Bt + Crd) and III (Ms + Qtz + Crd + Bt) plotted in an AFM diagram projected from muscovite, quartz, and vapor. A = Appin Phyllite. B = Ballachulish Slate and Transition Series. L = Leven Schist. For specimens 137 and 176 in zone II, dotted lines join analyzed chlorite-biotite compositions to *inferred* cordierite compositions (because the cordierite in these specimens was pinitized); the inferred cordierite compositions were determined by drawing a line from the biotite composition parallel to the Crd-Bt tie lines of the other specimens. In specimens 163 and 226 from zone III, dashed lines connect Crd-Bt compositions to chlorite that texturally appears to be secondary. The arrow indicates the direction of movement of Mg/(Mg + Fe) tie lines going through Reaction 1 (Ms + Chl + Qtz = Crd + Bt + H_2O).

causes their anomalously Mg-rich compositions, and consequently the Mg-rich composition of the coexisting cordierite, rather than vice versa. Otherwise, one would expect to see in samples containing the most magnesian biotite the highest F content; this pattern is not seen. For example, in Figure 3d, D620 is more magnesian than the F-rich specimen D515, but contains negligible F itself; the magnesian composition of D620 is fully rationalized by the movement of Mg/(Mg + Fe) tie lines through divariant Reaction 4b.

In pelitic rocks, F fractionates into hydrous minerals such as muscovite and, especially, biotite and is thought to be a remnant from the original premetamorphic sedimentary protolith. During prograde metamorphism, dehydration reactions that consume muscovite and/or biotite will concentrate the F into the remaining mica (Valley et al., 1982). However, the facts that (1) many specimens from the highest-grade zones (Va and Vb) contain biotite with negligible F and (2) a number of specimens at low grades contain significant F point to its variation in the aureole being principally due to bulk compositional control rather than metamorphic grade (see Table 3).

It should be noted that all specimens in the aureole contain abundant biotite and/or muscovite, which is probably the main reason why primary bulk compositional variation overwhelms the influence of fractionation. This is in contrast to higher-grade granulites, which contain a lower modal abundance of biotite and show correspondingly higher F contents.

Variation in K_D (Fe-Mg) between cordierite and biotite

Figure 4 plots the variation in K_D $[(Mg/Fe)_{Bt}/(Mg/Fe)_{Crd}]$ through the metamorphic zones. The values used to calculate K_D are obtained from Table 3. Even within individual zones, the variation is huge, and there is no significant pattern with grade. This is in contrast to the significant variation with temperature of K_D (Fe-Mg) between garnet-biotite (e.g., Ferry and Spear, 1978) and garnet-cordierite (e.g., Thompson, 1976). The difference in Mg/(Mg + Fe) between coexisting cordierite and biotite is small compared to the above two pairs involving garnet, so that the driving force for Fe-Mg partitioning is much smaller and correspondingly more significantly perturbed by local charge effects and coupled substitutions involving minor elements such as Na, Ca, Mn, Ti, Al, Fe^{3+}, and F in biotite and Na, Mn, Fe^{3+}, and H_2O in cordierite. For this reason, the K_D (Fe-Mg) between cordierite and biotite is of no use for geothermometry.

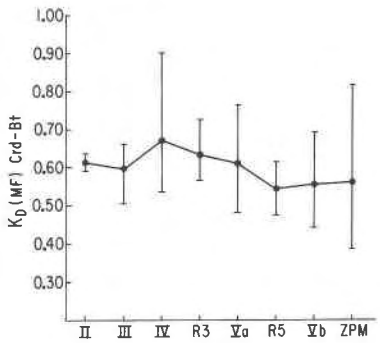

Fig. 4. Variation with grade of $K_D = (Mg/Fe)_{Bt}/(Mg/Fe)_{Crd}$. The heavy dots are the mean of the values from each zone, with the brackets indicating the range. Numerical data are listed in Table 3.

←

(b) Compositions of cordierite and biotite from zone IVb (Bt + Qtz + Crd + Kfs ± Ms), plotted in an AFM diagram projected from K-feldspar, quartz, and vapor. See Table 2 for the specimens that contain muscovite. Also shown are the compositions of coexisting cordierite and biotite from the three univariant Ms + Qtz + Al_2SiO_5 + Kfs + Crd + Bt assemblages (dotted area—R3). Several of the specimens were collected at grades higher than zone IVb, but are inferred to have had their assemblages and Mg/(Mg + Fe) compositions developed during passage through zone IVb (Reaction 2b: Ms + Bt + Qtz = Crd + Kfs + H_2O) (see Table 3 and text). The arrow indicates the movement of Mg/(Mg + Fe) tie lines going through Reaction 2b. A = Appin Phyllite. L = Leven Schist.

(c) Compositions of coexisting cordierite and biotite from zone IVa plotted in an AFM diagram projected from muscovite, quartz, and vapor. Also shown are the compositions of coexisting biotite and cordierite from the three univariant assemblages Ms + Qtz + Crd + Bt + Al_2SiO_5 + Kfs (dotted area—R3). B = Ballachulish Slate. L = Leven Schist. The arrow indicates the movement of Mg/(Mg + Fe) tie lines going through Reaction 2a (Ms + Crd = Qtz + Bt + Al_2SiO_5 + H_2O).

(d) Compositions of coexisting cordierite and biotite from zones V (Qtz + Bt + Al_2SiO_5 + Crd + Kfs) and Va (Ms + Bt + Al_2SiO_5 + Crd + Kfs) plotted in an SFM diagram projected from Al_2SiO_5, K-feldspar, and vapor (S = SiO_2 + $6K_2O$ + Al_2O_3. F = FeO + MnO. M = MgO). Also plotted are the compositions of coexisting cordierite and biotite from the univariant assemblages Ms + Qtz + Al_2SiO_5 + Kfs + Crd + Bt (R3) and Ms + Crn + Bt + Al_2SiO_5 + Crd + Kfs (R5) (dotted areas). A = Appin Phyllite. A(+F) = Appin Phyllite specimens that have biotite with >0.6 wt% F. L = Leven Schist. The arrows indicate the direction of migration of Mg/(Mg + Fe) tie lines going through quartz-bearing Reaction 4a (Qtz + Bt + Al_2SiO_5 = Crd + Kfs + H_2O) and quartz-absent Reaction 4b (Ms + Crd = Bt + Al_2SiO_5 + Kfs + H_2O).

(e) Compositions of coexisting cordierite and biotite from zone Vb (Bt + Al_2SiO_5 + Crn + Crd + Kfs) plotted in an SFM diagram projected from Al_2SiO_5, K-feldspar, and vapor. Also plotted are the compositions of cordierite and biotite from univariant assemblage Ms + Crn + Kfs + Al_2SiO_5 + Crd + Bt (dotted area—R5). The arrow indicates the direction of migration of Mg/(Mg + Fe) tie lines going through Reaction 6 (Bt + Al_2SiO_5 = Crn + Crd + Kfs + H_2O). Some specimens included in zone Vb come from within the zone of partial melting, but contain no textures that suggest partial melting within the specimens themselves.

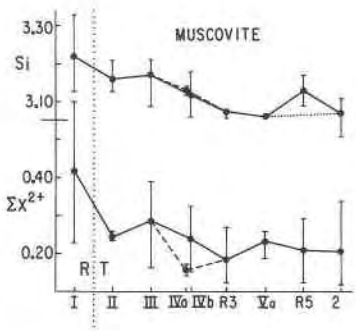

Fig. 5. Variation with grade of Si and ΣX^{2+} (=Fe + Mg + Mn + Ca) in muscovite from all units. For each zone, the mean is indicated by a point, and the range is indicated by the brackets. Roman numerals = metamorphic zones from Fig. 1 and elsewhere in the text. R3, R5 = Reactions 3 (Ms + Qtz = Al_2SiO_5 + Kfs + H_2O) and 5 (Ms = Crn + Kfs + H_2O). 2 = secondary muscovite from high-grade zones. R = regional metamorphism. T = thermal metamorphism. The line to zone IVa has been dashed to distinguish it from zone IVb, which occurs at the same grade. The dotted line in the Si trend going from zone Va to 2 is drawn because of doubts about the anomalously high Si values in R5. Numerical data listed in Table 3.

Tschermaks exchange: (Fe,Mg)Si = 2Al

The following sections focus on the importance of the Tschermaks exchange [(Fe,Mg)Si = 2Al] in coexisting micas in the Ballachulish area. These sections are arranged to (1) illustrate the simultaneous operation of the exchange (Fe,Mg)Si = 2Al in coexisting micas in different assemblages at different grades, (2) demonstrate the advantages of treating this exchange as a reaction vector in the sense of J. B. Thompson (1982a, 1982b), and (3) provide a theoretical rationale for the construction of P-T and isobaric T-$X_{Al\text{-}Si}$ diagrams involving (Fe,Mg)Si = 2Al. The T-$X_{Al\text{-}Si}$ diagram, when applied to pelitic rocks from Ballachulish, neatly accounts for their observed modal and chemical variations.

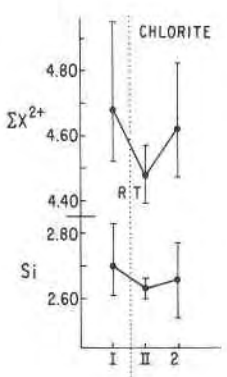

Fig. 6. Variation with grade of Si and ΣX^{2+} (=Fe + Mg + Mn + Ca) in chlorite from all units. Roman numerals refer to the metamorphic zones used in Fig. 1, Table 1, and elsewhere in the text. 2 = secondary chlorite. R = regional metamorphism. T = thermal metamorphism. For each zone, the mean value is indicated by a point, and the range is indicated by the brackets. Numerical data are listed in Table 3.

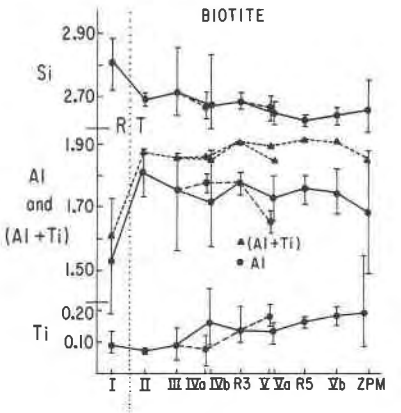

Fig. 7. Variation with grade of Si, Al, Ti, and Al + Ti in biotite from all units. ZPM = Zone of partial melting; all other symbols the same as in Figs. 5 and 6. The lines joining zones IVa and V to the overall trend have been dashed to distinguish them from zones IVb and Va, which occur at the same grade. Numerical data are listed in Table 3.

In theory, the extent of Tschermaks exchange [(Fe,Mg)Si = 2Al] in minerals may be monitored by the variation of the Si content, the Al content, or total divalent cations, provided that corrections can be made for Fe^{2+}-Fe^{3+} variation and that no other substitutions operate simultaneously in the minerals that may affect these quantities. In practice, particularly for micas, it has not been possible to consistently estimate Fe^{2+}/Fe^{3+} ratios from considerations of charge balance and ideal stoichiometry, and other substitutions, such as Fe^{3+} and Ti for Al in biotite, are important (Guidotti, 1984). Consequently, the most reliable gauge to the extent of (Fe,Mg)Si = 2Al, which is least affected by substitutional and charge-balance uncertainties, is the variation in Si content (see Miyashiro and Shido, 1984, for a fuller discussion).

Listed in Table 3 and illustrated in Figures 5–7 are the variations with grade in the Ballachulish aureole of Si content of chlorite, muscovite, and biotite. Additionally listed in Table 3 is the variation of Mg/(Mg + Fe) for all

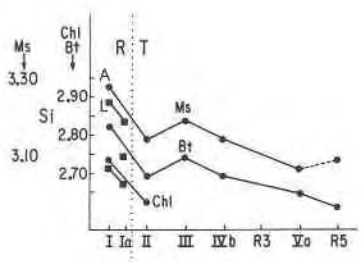

Fig. 8. Comparison of the variation with grade of Si in muscovite, biotite, and chlorite in the Appin Phyllite (contact metamorphism = heavy dots) and the Leven Schist (regional metamorphism = squares). The symbols are the same as used in Figs. 5–7.

the minerals, total divalent cations for chlorite and muscovite, and Al, Ti, and F^- for biotite. Because of the difficulty in determining Fe^{3+}/Fe^{2+} from ideal-site-occupancy considerations, all Fe is assumed to be Fe^{2+}.

It is important to note that no distinction is made among the three different sedimentary units in Figures 5–7; because the proportion of specimens from each of the units varies in each metamorphic zone, there is a superimposed bulk compositional effect on the illustrated trends. Specifically, the Ballachulish Slate overall contains the most aluminous chlorite, muscovite, and biotite, whereas the Appin Phyllite contains the most siliceous (see Table 3). In an effort to remove this bulk compositional effect, Figure 8 plots the variation in Si content of coexisting chlorite, muscovite, and biotite from specimens in the Appin Phyllite, the unit that is best represented at all grades.

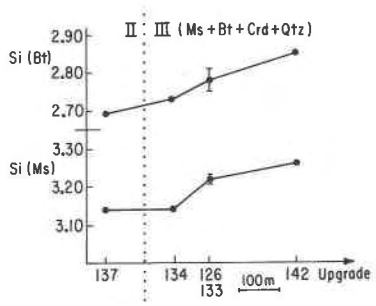

Fig. 9. Up-grade variation in Si content of coexisting biotite and muscovite from five specimens in the Appin Phyllite in Gleann Am Fhiodh (see Fig. 3). The specimens were projected into a line drawn due west from D137 in Fig. 1 to give the relative spacings. Numerical data are listed in Table 3. Roman numerals refer to metamorphic zones.

Muscovite

Primary muscovite from all units at regional grade has an average Si content of 3.22 (3.27 in the Appin Phyllite). Within regional-grade specimens in the Leven Schist, the Si content drops from 3.25 to 3.19 going from the chlorite ± biotite zone to the garnet zone, a change in regional metamorphic grade that represents primarily an increase in temperature (see above). Muscovite from within the thermal aureole is less Si-rich than in the regional grade rocks, with the Si content generally decreasing from about 3.17 in zone II to 3.06 at the highest grades. The Si content of secondary muscovite from several high-grade specimens, which is of retrograde origin, averages 3.07; this is comparable to the Si content of primary muscovite above zone IVb.

The pattern of ΣX^{2+} variation, although within larger range brackets, generally follows the Si pattern, which suggests that (Fe,Mg)Si = 2Al is the dominant substitutional reaction in the muscovite.

Chlorite

The Si content of primary chlorite drops from 2.70 to 2.61 going from regional grade rocks to zone II within the thermal aureole (2.74 to 2.63 in the Appin Phyllite). The average Si content of secondary chlorite from higher-grade rocks falls between these values. Within regional grade specimens in the Leven Schist, the Si content drops from 2.72 to 2.68 going from the chlorite ± biotite zone to the garnet zone. The absolute magnitude of the Si variation in chlorite is less than in muscovite, although the direction of change is the same. As with muscovite, the Σ^{2+} pattern is subparallel to the Si pattern.

Biotite

Regional-grade biotite has an average Si content of 2.80 (2.83 in the Appin Phyllite). In the Leven Schist, going from the chlorite ± biotite zone to the garnet zone, the Si content drops from 2.83 to 2.75. Within the thermal aureole, the Si content decreases from 2.67 in zone II, increases to 2.71 to zone III, and then decreases to 2.61–2.65 in the highest-grade zones. The direction and magnitude of these changes is very similar to the muscovite pattern.

With the exception of specimens from low-grade zones below zone IVb, the Al content does not vary inversely with Si content, as one would expect if the exclusive exchange were (Fe,Mg)Si = 2Al. The Ti content of biotite significantly increases with grade above zone III, as has been observed in other terranes by numerous workers (see Guidotti, 1984, for a review). Above zone III, the variation of (Al + Ti) more closely represents an inverse relationship with Si (see Fig. 7), which suggests the operation of the exchange reaction

$$^{VI}Ti^{4+} + 2^{IV}Al^{3+} = {}^{VI}(Fe,Mg)^{2+} + 2^{IV}Si^{4+}.$$

This reaction was identified by Tracy (1978) to be the most important Ti-substitutional reaction in biotite from high-grade pelitic rocks from Massachusetts. Stoichiometrically, the reaction is related to the simpler Tschermaks exchange, (Fe,Mg)Si = 2Al.

Within each metamorphic zone, the most magnesian biotites tend to be the most Si-rich, but this is not a strong trend and there are numerous exceptions (e.g., D65, D63b, zone Vb: Mg/(Mg + Fe): 0.38, 0.77; Si: 2.66 in both). The pattern is most pronounced in biotite with Mg/(Mg + Fe) greater than 0.65 (see Table 3 and Guidotti, 1984, for a fuller discussion).

Comparison of Si variation between coexisting micas

Figure 8 compares the variation with grade of Si content in coexisting chlorite, muscovite, and biotite in regional-grade specimens from the Leven Schist and contact metamorphic specimens from the Appin Phyllite. The correlation is striking and demonstrates that the extent of (Fe,Mg)Si = 2Al in these minerals, particularly muscovite and biotite, varies sympathetically with grade through a wide range of assemblages.

Figure 9 illustrates the variation with grade of the Si content of coexisting muscovite and biotite in zones II (Ms + Chl + Bt + Crd + Qtz) and III (Ms + Bt +

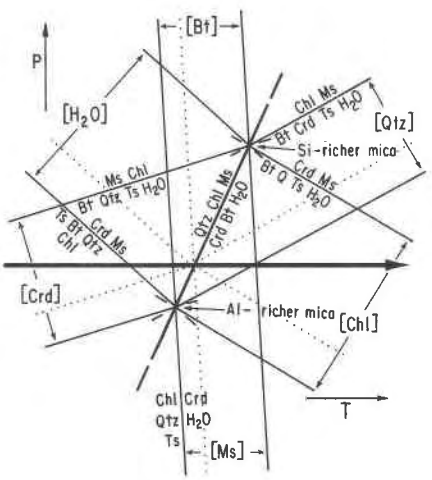

Fig. 10. Schematic Schreinemakers net showing the family of reactions involving (Fe,Mg)Si = 2Al that are related to the KMASH or KFASH univariant Reaction 1: Ms + Chl + Qtz = Crd + Bt + H_2O. The reactions are listed in Table 4. Although each of the reactions involving the Tschermaks exchange is divariant, for clarity the reactions have been labeled along one of the bounding curves of the divariant fields. These bounding curves represent isopleths of Si content of chlorite, muscovite, and biotite and are not endmember curves. On univariant Reaction 1, the Si contents of chlorite, muscovite, and biotite coincide, as indicated by the dotted lines (isopleths). The net is oriented in *P-T* space to be consistent with Powell and Evans's (1983) calibration of Ms + Chl = Bt + Qtz + Ts + H_2O (R1) and Seifert's (1970) data on Ms + Chl + Qtz = Crd + Bt + H_2O. The bold arrow represents the isobaric trajectory at Ballachulish.

Crd + Qtz) in specimens from the Appin Phyllite (see Fig. 1). Within zone III, uniquely defined by the assemblage Ms + Crd + Bt + Qtz, there is a consistent and parallel increase in Si content of coexisting muscovite and biotite with increasing grade (i.e., temperature).

The sympathetic trend of Si content in muscovite, chlorite, and biotite in Figures 8 and 9 suggests that (Fe,Mg)Si = 2Al operates simultaneously in all of the micas, rather than in only one. This is powerful, practical justification of the treatment of (Fe,Mg)Si = 2Al as a general exchange vector, in the sense of Thompson (1982a, 1982b).

$(Fe,Mg)_{-1}$ Si_{-1} Al_2 as a reaction vector

Previously, a number of pelitic reactions, particularly those involving the first appearance of biotite in low-grade Ms + Chl + Qtz pelites, have been written in a form such as

$$\text{phengitic Ms} + \text{Chl} = \text{less phengitic Ms} + \text{Bt} + \text{Qtz} + H_2O \quad (7)$$

and

$$\text{phengitic Ms} + \text{Kfs} + \text{Chl} = \text{less phengitic Ms} + \text{Bt} + \text{Qtz} + H_2O, \quad (8)$$

both from Mather (1970). The form of both these reactions focuses on (Fe,Mg)Si = 2Al in muscovite only; this is in contrast to Figures 8 and 9, in which it is clear that (Fe,Mg)Si = 2Al operates in all of the micas.

J. B. Thompson (1982a, 1982b) has described the advantages of assessing the possible range of reactions in a given system of phases and components by selecting additive components and exchange vectors. Confining the discussion to the system K_2O-MgO-Al_2O_3-SiO_2-H_2O (KMASH) and the phases muscovite (sensu lato), chlorite, biotite, quartz, and vapor, suitable additive components are $KAl_3Si_3O_{10}(OH)_2$, $Mg_5Al_2Si_3O_{10}(OH)_8$, $KMg_3AlSi_3O_{10}(OH)_2$, SiO_2, and H_2O, respectively; the only important exchange vector is $Mg_{-1}Si_{-1}Al_2$ (MgSi = 2Al, the Tschermaks exchange). Net-transfer Reaction 7, written using the above components, is

$$\underset{\text{muscovite}}{3KAl_3Si_3O_{10}(OH)_2} + \underset{\text{chlorite}}{Mg_5Al_2Si_3O_{10}(OH)_8} = \underset{\text{biotite}}{3KMg_3AlSi_3O_{10}(OH)_2} + \underset{\text{Tschermaks exchange}}{4Mg_{-1}Si_{-1}Al_2} + \underset{\text{quartz}}{7SiO_2} + \underset{\text{water}}{4H_2O}. \quad (9)$$

TABLE 4. Summary of reactions involving Ms + Bt + Chl + Qtz + Crd + H_2O and the Tschermaks exchange (Ts: $Mg_{-1}Si_{-1}Al_2$)

Reaction components:	Ms Chl Qtz Crd Bt Ts H_2O = 7
	Note: Ts = [$Mg^{2+}Si^{4+}$ = Al^{3+}] = $Mg_{-1}Si_{-1}Al_2$
System components:	KMASH = 5
Univariant reactions: 1	Ms + Chl + Qtz = Crd + Bt + H_2O*
Divariant reactions: 6	
[Ts]	Ms + Chl + Qtz = Crd + Bt + H_2O*
[Ms, Bt]	Chl + Qtz + Ts = Crd + H_2O
[Chl]	Bt + Qtz + Ts + H_2O = Ms + Crd
[Crd]	Ms = Chl = Bt + Qtz + Ts + H_2O
[Qtz]	Ms + Chl = Bt + Crd + Ts + H_2O
[H_2O]	Bt + Qtz + Ts + Chl = Ms + Crd

Note: Reactions are designated by the absent reaction component(s).

* The Tschermaks-absent divariant reaction [Ts] is the same as the univariant reaction, because at any point on the univariant reaction the Tschermaks compositions of all the minerals are uniquely defined, and there is therefore no reaction due to the Tschermaks exchange.

This method of writing the reaction emphasizes the role of (Fe,Mg)Si = 2Al(MgSi = 2Al in KMASH) as a general exchange component that is not confined to any particular mineral. According to this reaction, muscovite and chlorite are consumed to produce biotite, quartz, and vapor, with chlorite, biotite, and muscovite becoming more Al-rich as the reaction proceeds.

Schreinemakers analysis of reactions involving (Fe,Mg)Si = 2Al

A. B. Thompson (1982), after J. B. Thompson (1979), pointed out that, for each univariant reaction involving muscovite and/or biotite in KMASH (or KFASH), there is a family of related pseudodivariant reactions involving MgSi = 2Al (or FeSi = 2Al). This is analogous to the family of divariant Fe-Mg reactions in KFMASH that are related to a univariant reaction. The term pseudodivariant is used because the exchange vector $(Fe,Mg)_{-1}Si_{-1}Al_2$ is not a true phase, but may be regarded as an independent exchange component.

As an example of this approach, consider Reaction 1, Ms + Chl + Qtz = Crd + Bt + H_2O, which is univariant in KMASH or KFASH. The family of pseudodivariant reactions involving (Fe,Mg)Si = 2Al is listed in Table 4, and a schematic Schreinemakers net of these reactions is illustrated in Figure 10. This diagram has been approximately oriented in P-T space using Powell and Evans's (1983) thermodynamic calibration of Reaction 9 and Seifert's (1970) experimental calibration of Reaction 1; all other reaction topologies are speculative.

Along the KMASH univariant reaction (Ms + Chl + Qtz = Crd + Bt + H_2O), the Si contents of the chlorite, muscovite, and biotite change, with the consequence that the coefficients of the reaction will change. As noted by Seifert (1970) and A. B. Thompson (1982), this makes the P-T evaluation of such a reaction, involving micas, very difficult. At any point on the univariant reaction, the Si contents of the chlorite, muscovite, and biotite are uniquely defined (see the dotted lines in Fig. 10), just as in KFMASH the Mg/(Mg + Fe) compositions of coexisting ferromagnesian phases are uniquely defined at a univariant curve (A. B. Thompson, 1982).

In this discussion, Tschermaks exchange reactions between coexisting chlorite, muscovite, or biotite—such as Si-rich Ms + Al-rich Chl = Al-rich Ms + Si-rich Chl—have been ignored. This is equivalent to ignoring Fe-Mg exchange between coexisting ferromagnesian phases, e.g., cordierite and biotite, when examining Fe-Mg variation of these minerals through the aureole (see above).

T-$X_{Al\text{-}Si}$ diagram

In Figure 10 a bold arrow has been drawn that represents the isobaric prograde path through the thermal aureole. Applying similar reasoning used in the construction of an isobaric T-$X_{Fe\text{-}Mg}$ diagram for the Fe-Mg divariant reactions discussed above, an isobaric T-$X_{Al\text{-}Si}$ diagram may be constructed that illustrates the importance of Al-Si variation in controlling the development and chemical variation of assemblages in the aureole (see Fig. 11). The relative ranking in Si/(Si + Al) ratios of natural chlorite, muscovite, and biotite is Bt > Ms > Chl (Pattison, 1985; Deer et al., 1966). In this diagram, only (Fe,Mg)Si = 2Al is being considered, so that the relative Si/(Si + Al) ratios between the minerals remain constant.

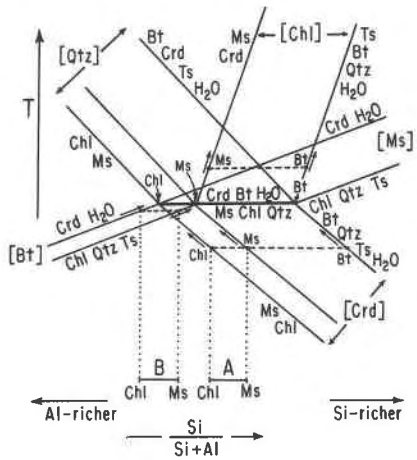

Fig. 11. Schematic isobaric T-$X_{Al\text{-}Si}$ diagram for the pressure trajectory in Fig. 10 (refer to Table 4 and Fig. 10 for the reactions). The above topology and movement of the lines has been drawn to be consistent with the observed Si/(Si + Al) variation of coexisting Ms + Bt ± Chl in the Ballachulish assemblages (see Figs. 5–9, Table 5, and text). Two pairs of coexisting Chl and Ms with differing Si/(Si + Al) ratios (A and B) are drawn to illustrate the contrast in evolution of their Si contents with increasing grade (see text). The short dashed lines represent tie lines between Ms ± Chl ± Bt in different assemblages. The small arrows indicate the direction of migration of the Si/(Si + Al) content of the coexisting micas as the different reactions proceed.

Referring to Figure 11, consider two starting compositions, A and B, containing muscovite and chlorite. For composition A, as temperature rises, Reaction 9 (Ms + Chl = Bt + Qtz + Ts + H_2O) is encountered, and the chlorite and muscovite will begin to react to produce biotite. As temperature continues to rise, more muscovite and chlorite are consumed to produce more biotite, with all of the micas becoming more aluminous. At univariant Reaction 1 (Ms + Chl + Qtz = Crd + Bt + H_2O), cordierite is produced, and the Si contents of these minerals are fixed until chlorite, muscovite, or quartz is consumed. If quartz is consumed, then the quartz-absent pseudodivariant reaction is entered, and chlorite and muscovite will react to produce biotite and cordierite, with all of the micas becoming more aluminous as temperature rises. If chlorite is consumed, then the chlorite-absent pseudodivariant reaction is entered (as illustrated in Fig. 11).

In contrast, composition B will enter the biotite-absent pseudodivariant reaction, Chl + Qtz + Ts = Crd + H_2O, producing cordierite while the muscovite and chlorite becomes more Si-rich. With rising temperatures, Reaction 1 will be encountered where the Si contents of the micas are the same as for starting composition A.

TABLE 5. Average Si contents of coexisting chlorite, muscovite, and biotite in low-grade pelites

Assemblage	Chl	Mu	Bi
Ms + Chl + Qtz	2.62	3.16	
Ms + Chl + Bt + Qtz	2.75	3.27	2.85
Ms + Chl + Bt + Grt + Qtz	2.63	3.21	2.76
Ms + Chl + Qtz + Bt + Crd	2.65	3.18	2.70

Note: Individual data are listed in Table 3.

Application of the T-$X_{Al\text{-}Si}$ diagram to pelites in the Ballachulish area

Table 5 lists the average Si content of coexisting muscovite, chlorite, and biotite from the assemblages Ms + Chl + Qtz, Ms + Chl + Bt + Qtz (both in zone I), Ms + Chl + Bt + Grt + Qtz (zone Ia), and Ms + Chl + Qtz + Bt + Crd (zone II). The first three assemblages were formed during regional metamorphism, with the latter assemblage being a contact metamorphic assemblage. This conclusion is based on the spatial distribution of the first three assemblages being unrelated to their proximity to the igneous complex (Pattison, 1985). Figure 11, although drawn for cordierite-bearing reactions (i.e., thermal metamorphic conditions), may be adapted to the regional-grade assemblages simply by replacing cordierite with garnet (the reaction stoichiometries will change but the form of the diagram is preserved).

Three examples from the Ballachulish area demonstrate the application of the T-$X_{Al\text{-}Si}$ diagram.

1. In regional-grade assemblages in the Ballachulish Slate, biotite is never present; the only observed assemblage is Ms + Chl + Qtz. This is in contrast to the Appin Phyllite and Leven Schist, in which biotite is present in the regional-grade assemblages Ms + Chl + Bt + Qtz and Ms + Bt + Qtz + Grt ± Chl. The absence of biotite in the Ballachulish Slate cannot be explained by variations in bulk rock Mg/(Mg + Fe), because there is considerable overlap in Mg/(Mg + Fe) of chlorite in biotite-absent specimens (e.g., D157, 164) and biotite-bearing specimens (e.g., D16, 92). The graphitic nature of the slate cannot be the reason for the absence of biotite, because the addition of C-bearing species to the fluid phase lowers a_{H_2O} and would therefore promote the biotite-forming reaction (Ms + Chl = Bt + Ts + Qtz + H_2O) relative to graphite-free units. Examining Table 5, it is clear that biotite-absent assemblages are the most aluminous, so that the restriction of Bt-absent assemblages to the Ballachulish Slate may simply be explained by its being more aluminous. Figure 11 schematically illustrates this, with "B" representing Ballachulish Slate and "A" representing Appin Phyllite and Leven Schist. Significantly, the average Si content of coexisting micas in regional garnet-bearing specimens has decreased from the average Si content of micas in the lower-grade specimens containing only biotite, which suggests progress of Reaction 9 up to the garnet-producing reaction (illustrated in Fig. 11 if "Grt" is substituted for "Crd").

2. The Si contents of coexisting Ms and Chl in the assemblages Ms + Chl + Qtz and Ms + Chl + Bt + Qtz ± Grt converge at contact metamorphic Reaction 1 (Ms + Chl + Qtz = Crd + Bt + H_2O) (see Table 5); the more Si-rich biotite-bearing assemblages become *less* Si-rich, while the more Si-poor biotite-absent assemblages become *more* Si-rich. Referring to Figure 11, in the Si-poor, Bt-absent assemblage Ms + Chl + Qtz typically developed in the Ballachulish Slate, Ms and Chl become more Si-rich by the operation of the reaction Chl + Qtz + Ts = Crd + H_2O. This suggests that a minor amount of cordierite may have been produced in Ms + Chl assemblages prior to its major development with biotite in Reaction 1. As Bt-bearing assemblages approach Reaction 1, the Si content of coexisting micas decreases by the reaction Ms + Chl = Bt + Ts + Qtz + H_2O. At Reaction 1, the Si contents of the micas, regardless of the prior assemblage, are approximately the same, as predicted by Figure 11.

3. Above Reaction 1 (zone II in the aureole) is a relatively broad zone (zone III) in which the trivariant assemblage Ms + Bt + Qtz + Crd persists. Within this assemblage, in specimens that are progressively closer to the contact (and were therefore at progressively higher temperature), the Si content of coexisting biotite and muscovite steadily increases (see Fig. 9). Referring to Figure 11, this may be explained by the up-temperature passage through the chlorite-absent pseudodivariant reaction Bt + Qtz + Ts + H_2O = Ms + Crd. Petrographically, this reaction is consistent with the increased abundance and size of cordierite in zone III compared to that in zone II.

If cordierite at this low grade contains structurally bound H_2O, which it most probably does, judging from the low microprobe totals and the experimental results of Mirwald and Schreyer (1977), then vapor becomes a reactant phase too. The prograde consumption of vapor, although unusual, need not prohibit the operation of this "minor" reaction, since all of the "major" reactions in the aureole are dehydration reactions, which may be expected to keep a_{H_2O} in the pelites high. In addition, there is clear petrographic evidence, also within zone III of the thermal aureole, of the formation of regional-grade pseudomorphs of cordierite and biotite after garnet via the reaction Ms + Gt + Qtz + H_2O = Crd + Bt. Assuming cordierite to be hydrous, then vapor must also be a reactant phase in this reaction. Newton and Wood (1979) have also discussed the occurrence of some prograde vapor-consuming, cordierite-producing reactions.

Expansion from KMASH to KFMASH

When the scope of the T-$X_{Al\text{-}Si}$ diagram is extended from KMASH to KFMASH, the univariant reaction Ms + Chl + Qtz = Crd + Bt + H_2O becomes divariant, and the pseudodivariant reactions involving Tschermaks exchange become pseudotrivariant. Unfortunately, in the field, zone II is so narrow that there were insufficient specimens collected within it to determine whether the

Si content of coexisting chlorite, muscovite, and biotite increases or decreases with grade.

Because the Si content of micas generally decreases with increasing grade, it seems likely that within Reaction 1, and in other comparable divariant reactions, the Si content decreases. Miyashiro and Shido (1984) demonstrated that within the reaction Ms + Chl + Qtz = Grt + Bt + H_2O, as the Chl, Grt, and Bt moved to more magnesian compositions, the Chl, Ms, and Bt became less Si-rich. At higher grade, with the appearance of staurolite, there was no observable change in Si content of the three minerals. This is consistent with the observations of this study that there appears to be a lower limit of Si content in muscovite (3.07) and biotite (2.68) that is reached by Reaction 3 (Ms + Qtz = Al_2SiO_5 + Kfs + H_2O; ~640°C at 3 kbar) (Pattison, 1985; see Figs. 5 and 6). As the grade increases, the Si content of the micas remains approximately constant.

Conclusions

1. With the exception of specimens from the graphitic Ballachulish Slate and those containing F-rich biotite, the theoretical prediction of the movement of Mg/(Mg + Fe) tie lines passing through the sequence of prograde discontinuous and continuous reactions in the Ballachulish aureole is consistent with the measured values from the different zones. The Fe-Mg distribution coefficient between biotite and cordierite, $K_D[(Mg/Fe)_{Bt}/(Mg/Fe)_{Crd}]$, does not vary significantly with grade and is therefore of no use for geothermometric calculations.

2. The F content of biotite affects the Mg/(Mg + Fe) ratios of coexisting biotite and cordierite by stabilizing biotite, and consequently cordierite, to anomalously Mg-rich compositions. Overall, primary bulk compositional variation is the most important control on the F content of biotite in the aureole, rather than metamorphic grade.

3. The Tschermaks exchange, (Fe,Mg)Si = 2Al, operates simultaneously in coexisting chlorite, muscovite, and biotite going through the different metamorphic zones, which highlights the importance of treating this substitutional reaction as a general exchange vector in the sense of J. B. Thompson (1982a, 1982b). Related to each mica-bearing univariant reaction in KMASH or KFASH is a family of pseudodivariant reactions involving (Fe,Mg)Si = 2Al, which may be evaluated using Schreinemakers analysis. Isobaric T-$X_{Al\text{-}Si}$ diagrams, analogous to T-$X_{Fe\text{-}Mg}$ diagrams, may be constructed to demonstrate how variations in the Al/(Al + Si) compositions of chlorite and muscovite in low-grade phyllites control the development of low-grade biotite-bearing assemblages, and to account for the variation with grade of the Si content of coexisting micas in a variety of assemblages.

Acknowledgments

This work forms part of a Ph.D. thesis completed at Edinburgh University. I especially thank Ben Harte, who provided me with excellent supervision. I acknowledge the Association of Commonwealth Universities for funding my Ph.D. at Edinburgh through a Commonwealth Scholarship, and NSF Grant EAR 84-11192 to R. C. Newton for publication assistance. I thank Ted Labotka, Alex Speer, Bob Newton, and an anonymous reviewer for their comments on the manuscript, and Cassandra Spooner for patiently typing the manuscript.

References

Bailey, E.B., and Maufe, H.B. (1960) The geology of Ben Nevis and Glen Coe and the surrounding country: Explanation of Sheet 53, Memoir of the Geological Society of Scotland, H.M.S.O., Edinburgh.

Brown, P.E., Miller, J.A., Soper, N.J., and York, D. (1968) Potassium-argon age pattern of the British Caledonides. Yorkshire Geological Society Proceedings, 35, 103–138.

Deer, W.A., Howie, R.A., and Zussman, J. (1966) An introduction to the rock forming minerals. Longman, London, 528 p.

Evans, N.H., and Speer, J.A. (1984) Low pressure metamorphism and anatexis of Carolina Slate Belt phyllites in the contact aureole of the Lilesville pluton, North Carolina, U.S.A. Contributions to Mineralogy and Petrology, 87, 297–309.

Ferry, J.M., and Spear, F.S. (1978) Experimental calibration of the partitioning of Fe and Mg between biotite and garnet. Contributions to Mineralogy and Petrology, 66, 113–118.

Guidotti, C.V. (1984) Micas in metamorphic rocks. Mineralogical Society of America Reviews in Mineralogy, 13, 357–368.

Guidotti, C.V., Cheney, J.T., and Conatore, P.D. (1975) Coexisting cordierite + biotite + chlorite from the Rumford quadrangle, Maine. Geology, 3, 147–148.

Harmon, R.S. (1983) Oxygen and strontium isotopic evidence regarding the role of continental crust in the origin and evolution of the British Caledonian granites. In M.P. Atherton and C.D. Gribble, Eds. Migmatites, melting and metamorphism. Shiva Publishing, Nantwich, Cheshire, 62–79.

Heinrich, K.F.J. (1966) X-ray absorption uncertainty. In T.D. McKinley, K.F.J. Heinrich, and D.B. Wittey, Eds. The electron microprobe. Wiley, New York, 1035 p.

Kretz, R. (1983) Symbols for rock-forming minerals. American Mineralogist, 68, 277–279.

Labotka, T.C., Papike, J.J., and Vaniman, D.T. (1981) Petrology of contact metamorphosed argillite from the Rove Formation, Gunflint Trail, Minnesota. American Mineralogist, 66, 70–86.

Litherland, M. (1980) The stratigraphy of the Dalradian rocks around Loch Creran, Argyllshire. Scottish Journal of Geology, 16, 105–123.

Mather, J.D. (1970) The biotite isograd and the lower greenschist facies in the Dalradian rocks of Scotland. Journal of Petrology, 11, 253–275.

Miller, J.A., and Brown, P.E. (1965) Potassium-argon age studies in Scotland. Geological Magazine, 102, no. 2, 106–134.

Mirwald, P.W., and Schreyer, W. (1977) Die stabile und metastabile Abbaureaktion von Mg-cordierit in Talk, Disthen und Quartz und ihre Abhangigkeit vom Gleichwichts wassergehalt des Cordierits. Fortschritte der Mineralogie, 55, 95–97.

Miyashiro, A., and Shido, E. (1984) Tschermak substitution in low- and middle-grade pelitic schists. Journal of Petrology, 26, no. 2, 449–487.

Munoz, J.L. (1984) F-OH and Cl-OH exchange in micas with applications to hydrothermal ore deposits. Mineralogical Society of America Reviews in Mineralogy, 13, 469-544.

Newton, R.C., and Wood, B.J. (1979) Thermodynamics of water in cordierite and some petrological consequences of cordierite as a hydrous phase. Contributions to Mineralogy and Petrology, 68, 391–405.

Pattison, D.R.M. (1985) Petrogenesis of pelitic rocks in the Ballachulish thermal aureole. Thesis, University of Edinburgh, 590 p.

Pattison, D.R.M., and Harte, B. (1985) A petrogenetic grid for pelites in the Ballachulish and other Scottish thermal aureoles. Journal of the Geological Society, 142, no. 1, 7–28.

Powell, R., and Evans, J.A. (1983) A new geobarometer for the assemblage biotite-muscovite-chlorite-quartz. Journal of Metamorphic Geology, 1, 331–336.

Roberts, J.L. (1976) The structure of the Dalradian rocks in the North Ballachulish district of Scotland. Geological Society of London Journal, 132, 139–154.

Schreinemakers, F.A.H. (1915–1925) In-, mono-, and divariant equilib-

ria. Koninklijke Nederlandse Akademie van Wetenschappen, Proceedings, 18–28.

Seifert, F. (1970) Low temperature compatibility relations of cordierite in haplopelites of the system K_2O-MgO-Al_2O_3-SiO_2-H_2O. Journal of Petrology, 11, 73–99.

Sweatman, T.R., and Long, J.V.P. (1969) Quantitative electron-probe microanalysis of rock-forming minerals. Journal of Petrology, 10, 332–379.

Thompson, A.B. (1976) Mineral reactions in pelitic rocks: I. Prediction of *P-T-X*(Fe-Mg) phase relations. II. Calculation of some *P-T-X*(Fe-Mg) phase relations. American Journal of Science, 276, 401–454.

——— (1982) Dehydration melting of pelitic rocks and the generation of H_2O undersaturated granitic liquids. American Journal of Science, 282, 1567–1595.

Thompson, J.B., Jr. (1979) The Tschermak substitution and reactions in peltitic schists. In V.A. Zharikov, V.I. Fonarev, and S.P. Korikovshii, Eds. Problems in physiochemical petrology (in Russian). Moscow Academy of Science, 146–159.

——— (1982a) Composition space: An algebraic and geometric approach. Mineralogical Society of America Reviews in Mineralogy, 10, 1–32.

——— (1982b) Reaction space: An algebraic and geometric approach. Mineralogical Society of America Reviews in Mineralogy, 10, 33–52.

Tracy, R.J. (1978) High grade metamorphic reactions and partial melting in pelitic schist, west-central Massachusetts. American Journal of Science, 278, 150–178.

Treagus, J.E. (1974) A structural cross-section of the Moine and Dalradian rocks of the Kinlochleven area, Scotland. Geological Society of London Journal, 130, 525–544.

Troll, G., and Weiss, S. (1984) Petrographische und geothermometrische Untersuchungen am Ballachulish-complex (Schottland) (abs.). Fortschritte der Mineralogie, 62, 246–247.

Weiss, S. (1986) Petrogenese des Intrusivkomplexes von Ballachulish, Westschottland: Kristallisationverlauf in einen zonienten Kaledonischer pluton. Thesis, Universität München, 230 p.

Valley, J.W., Peterson, S.W., Essene, E.J., and Bowman, J.R. (1982) Fluorphlogopite and fluortremolite in Adirondack marbles and calculated C-O-H-F fluid compositions. American Mineralogist, 67, 545–557.

Manuscript received April 2, 1986
Manuscript accepted November 20, 1986